Effect of Orifice Surface Roughness on the Liquid Weeping in Bubble Columns

ARTICLE *in* INDUSTRIAL & ENGINEERING CHEMISTRY RESEARCH · NOVEMBER 2010

Impact Factor: 2.59 · DOI: 10.1021/ie101182x

5 AUTHORS, INCLUDING:

Raymond Lau
Nanyang Technological University
66 PUBLICATIONS **781** CITATIONS

SEE PROFILE

Effect of Orifice Surface Roughness on the Liquid Weeping in Bubble Columns

Md. Iqbal Hossain, Qing Xi Pang, Si Qi Pang, Yanhui Yang, and Raymond Lau*

Nangyang Technological University, Singapore, School of Chemical and Biomedical Engineering, 62 Nanyang Drive, Singapore 637459

Liquid weeping at the orifices of a gas distributor plate is one problem commonly encountered in bubble column operations. The effect of orifice surface roughness on the liquid weeping phenomenon in a bubble column is investigated over a superficial orifice gas velocity range of 143−703 cm/s. High-speed images of the bubbling and liquid weeping process are analyzed using a computer-aided image analysis algorithm. Pressure fluctuation in the plenum is also monitored. The liquid weeping rate is found to decrease with an increase in orifice surface roughness at low superficial orifice gas velocities while it increases with an increase in surface roughness at high superficial orifice gas velocities. Analysis indicates that the orifice surface roughness affects liquid weeping indirectly by changing the bubbling behaviors at the orifice. At low superficial orifice gas velocities, an increase in orifice surface roughness reduces the bubble size at bubble detachment. The reduction in pressure fluctuation in the plenum thus decreases the liquid weeping rate. On the other hand, as the superficial orifice gas velocity is approaching the bubbling/jetting regime transition, an increase in orifice surface roughness increases the transition velocity and hence the liquid weeping rate increases. Nonetheless, a modification of the orifice surface roughness is a viable solution to the liquid weeping problem in industrial bubble columns.

Introduction

Bubble columns are used in numerous chemical, petrochemical, biochemical, and metallurgical processes. Liquid weeping is a problem that is commonly faced in bubble column operations especially at low operating gas velocities. Liquid weeping refers to the flow of liquid from the column into the plenum section through the orifices upon bubble detachment. The presence of liquid weeping can cause plugging of orifices, uneven gas distribution and increased pressure drop across the gas distributor plate. Factors such as superficial orifice gas velocity, liquid physical properties, operating pressure, plenum volume, orifice diameter and thickness, orifice taperness, orifice number, and pitch distance on the gas distributor plate that affect liquid weeping have been extensively studied.[1−10] However, the effect of orifice surface roughness on liquid weeping in bubble columns is not available in the literature, though surface roughness has already been found to affect numerous scientific and engineering applications.[11−20]

It has been reported in our previous study that a bubble and liquid weeping cycle can be classified into four stages: bubbling, gas−liquid interface movement, weeping, and bridging.[5] As shown in Figure 1, the plenum pressure decreases in the bubbling stage because of the expansion of gas during bubble growth. The plenum pressure reaches a minimum when the bubble is just detached from the orifice and a new gas−liquid interface is formed. At this moment, the pressure at the top of the orifice is higher than the plenum pressure and the pressure difference would cause the gas−liquid interface to move toward the plenum. As the gas−liquid interface moves beyond the bottom of the orifice, liquid weeping occurs. The pressure in the plenum will increase during the gas−liquid interface movement and the weeping stages because gas is fed into the plenum continuously. When the plenum pressure reaches a critical pressure, $P_{c,critical}$, a sufficiently high plenum pressure to re-establish a gas−liquid interface at the bottom of the orifice, liquid weeping terminates. This re-establishment of the gas−liquid interface at the bottom of the orifice and its subsequent upward movement through the orifice until the initiation of the next bubble is termed as bridging.

The flow of liquid and gas in an orifice is analogous to the fluid flow in a pipe. If the fluid flow is under the laminar flow regime, the friction loss is independent of the surface roughness.[21] Under both transition and turbulent flow regimes, the friction loss of the fluid flow increases with an increase in surface roughness.[21] The rate of liquid weeping is closely related to the liquid weeping time and the pressure difference between the top of the orifice and the plenum pressure (driving force of liquid weeping). Because the orifice surface roughness can affect both of these factors, it is expected to have a significant effect on liquid weeping.

In this study, the effect of orifice surface roughness on liquid weeping in a bubble column is evaluated over a wide range of superficial orifice gas velocities. High-speed images of the bubbling and liquid weeping process at the orifices are analyzed using the image analysis algorithm developed in our previous study. The pressure fluctuation in the plenum is also monitored using a pressure transducer. The mechanisms underlying the effect of the orifice surface roughness on the liquid weeping phenomenon are proposed.

Experimental Section

The setup used in the experiment is shown in Figure 2. The bubble column is made of acrylic and has an internal diameter of 14 cm. The plenum volume is maintained at around 2300 $cm^3 \pm 70$ cm^3. Single circular orifice gas distributor plates are used. Each plate is made of acrylic and has a thickness of 0.5 cm. Single orifice gas distributor plates are used to prevent the disturbances from the bubbling process at neighboring orifices. The diameter of the orifice on all the distributor plates is kept at 0.5 cm to allow proper modification of the inner orifice surface. Compressed air is used as the gas phase whereas tap water is used as the liquid phase for each experimental run. An initial static liquid height of 40 cm is maintained in the column

* To whom correspondence should be addressed. Tel: +65 6316 8830. Fax: +65 6791 1761. E-mail:wmlau@ntu.edu.sg.

10.1021/ie101182x
Published on Web 11/30/2010

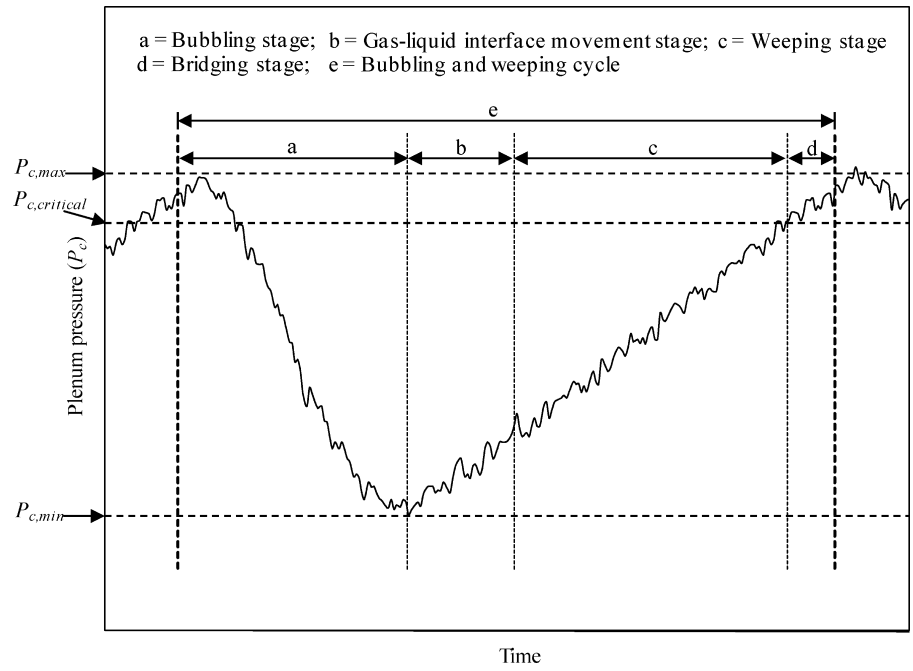

Figure 1. Illustration of plenum pressure fluctuation at different stages in a bubbling and weeping cycle.

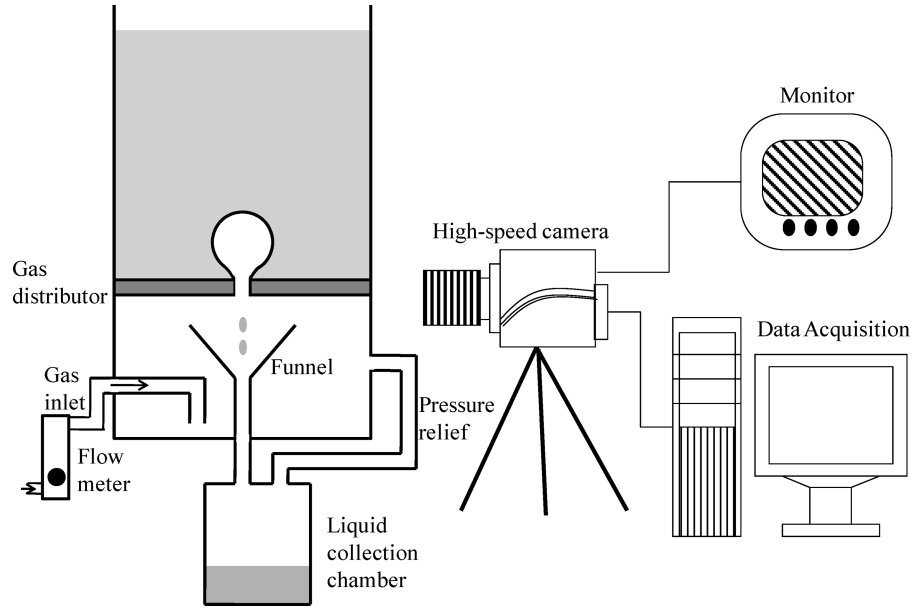

Figure 2. Experimental setup for liquid weeping measurements.

section for each experimental run. The superficial orifice gas velocity, defined as the average gas velocity at the orifice over the entire bubbling and liquid weeping cycle, is varied from 147 to 703 cm/s. The weeping liquid from the orifice is collected in a funnel placed in the plenum. A purge stream is used to aid the passing of the weeping liquid through the narrow channel of the funnel into the liquid collection chamber. The volume of the liquid weeping from the orifice over a certain period of operational time is measured to calculate the liquid weeping rate for each run. At least three experiments are conducted for each condition to ensure measurement repeatability. It is found that the variations in the weeping rates measured are less than 6% and a majority of the uncertainties are within 2% of the average weeping rate. A pressure transducer (Validyne DP-15) is installed at the plenum to monitor the pressure during the bubbling and liquid weeping process. A sampling frequency of 1000 Hz is used.

Five single orifice gas distributor plates, each with a different inner surface roughness, are used. The inner orifice surface of four distributor plates are treated with silicon carbide waterproof abrasive papers of grit sizes P100, P400, P800, and P1200 (FEPA specifications), respectively, after the orifice drilling step. The orifice surface treatment is performed by rotating the orifice plate at 600 rpm on a central lathe machine. The respective sand paper is attached onto a 4 mm circular steel rod and passes through the orifice of the rotating plate repeatedly. An additional polishing step is performed for the orifice plate treated with the P1200 abrasive paper by using polishing liquid (Brasso). The orifice surface of one distributor plate is kept untreated after the orifice drilling step. The roughness value of each inner surface is measured with a roughness testing system (Mitutoyo Surftester SV-3000 CNC), which consists of a sensory probe, a transducer, and a processor. The sensory probe is passed over the measurement surface to detect the up and down movement

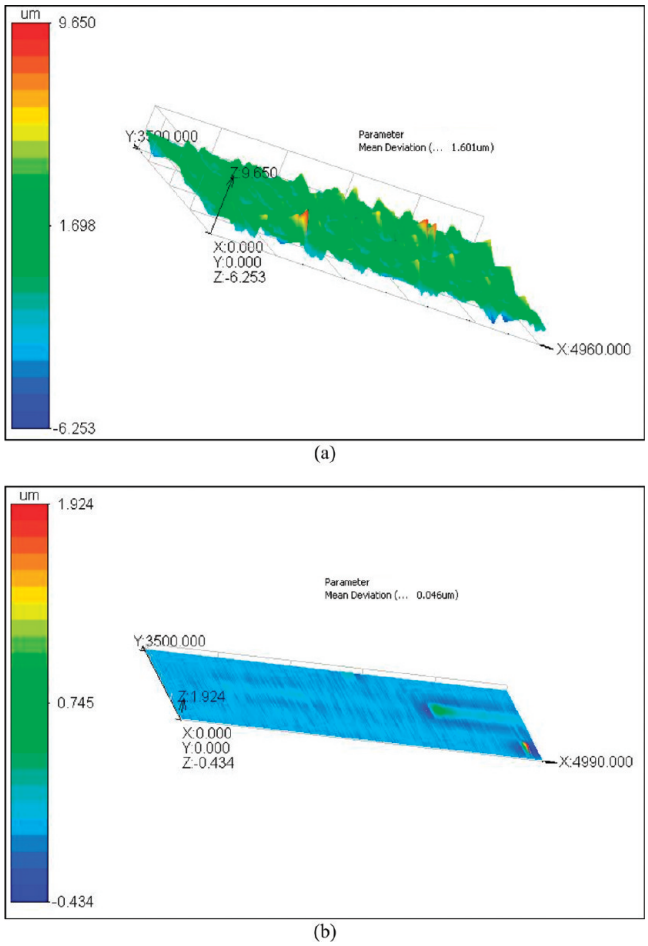

Figure 3. Visual roughness profile of the orifice inner surface: (a) untreated rough surface, (b) polished surface.

Table 1. Roughness Average Value for Different Orifice Surfaces

orifice inner surface treatment	RA (μm)
untreated	1.601
grit 100 sandpaper	1.262
grit 400 sandpaper	0.563
grit 800 sandpaper	0.353
grit 1200 sandpaper + polishing liquid	0.046

of the sensory probe. The signals detected by the transducer are then exported to a processor to convert the signals into a visual roughness profile. Sample visual roughness profiles for the untreated rough and the polished orifice surfaces considered in this study are shown in Figure 3. Inner surface roughness is quantified by the processor in terms of roughness average (RA). RA is the arithmetic average of the deviation of the roughness profile from its mean. The RA value for each orifice surface considered is shown in Table 1.

The bubbling and weeping process at the orifice is recorded by a high-speed video recording system (Olympus I-Speed) at a recording speed of 1000 Hz. The high-speed recording system consists of a high-speed camera, a monitor, and a data recording card. A 300 W halogen light is used as the illumination source. Image distortion due to the curvature in the column wall is found to be negligible when tested with reference square grids. An image analysis algorithm developed in our previous study is used to analyze the recorded image sequences to determine: (i) the time of each mechanistic stage in a bubbling and weeping cycle, and (ii) the emerging bubble volume.[5] The image analysis algorithm focuses on two regions of interest (ROI) obtained from an image frame. ROI-1 is immediately above the orifice

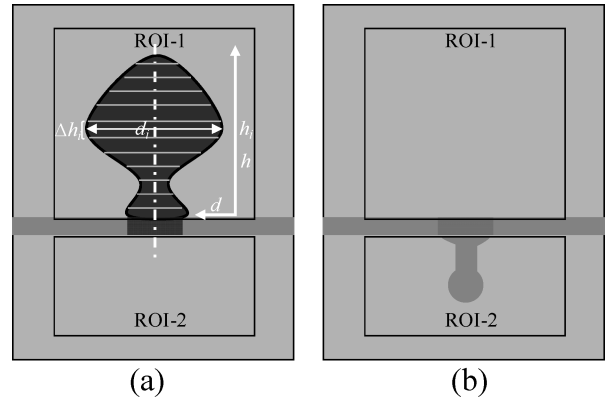

Figure 4. Illustration of the presence of emerging bubble and weeping liquid at the orifice during (a) bubbling, (b) liquid weeping, and (a) bubble volume determination.

Table 2. Illustration of Time Distribution Determination[a]

	Frame	ROI-1	ROI-2
	0	--	--
I	1	Connected bubble	--
I	2	Connected bubble	--
I	3	Connected bubble	--
I	4	Connected bubble	--
II	5	--	--
II	6	--	--
III	7	--	Weeping liquid
III	8	--	Weeping liquid
III	9	--	Weeping liquid
IV	10	--	--
IV	11	--	--
	12	Connected bubble	--

V

I = Bubbling stage; II = Gas-liquid interface movement stage; III = Weeping stage; IV = Bridging stage; V = Cycle.

[a] I = Bubbling stage; II = gas−liquid interface movement stage; III = weeping stage; IV = bridging stage; V = cycle.

plate to cover only the emerging bubble while ROI-2 is immediately below the orifice plate to cover only the weeping liquid as shown in Figure 4a and 4b. Both edge detection and region segmentation (Valley-Emphasis) methods are applied to each of these ROIs to identify the emerging bubble and weeping liquid from the respective ROIs. The presence of emerging bubble and weeping liquid in the ROIs of each frame are used as criteria to identify the mechanistic stages automatically in the algorithm based in Table 2. The emerging bubble volume can be determined by assuming that each horizontal differential element of a bubble is symmetric about its central vertical axis. As illustrated in Figure 4a, the contour of the bubble image can be discretized into a number of horizontal differential elements. The bubble volume can be estimated by the sum of all the volumes of the disks from rotating each differential

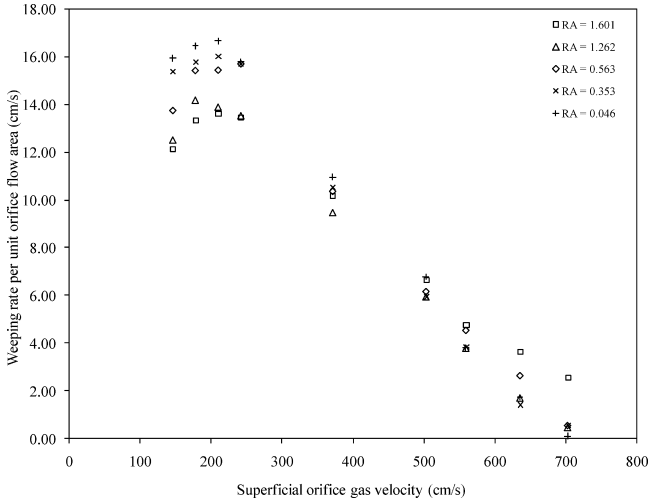

Figure 5. Effect of orifice surface roughness (RA, in μm) on liquid weeping rate.

element 360°. A mathematic representation of the operation can be written as

$$v_b = \sum_{i=1}^{N} \left(\frac{\pi}{4}\right) d_i^2 \Delta h_i \tag{1}$$

where N is the number of horizontal differential elements, Δh_i is the vertical height of the ith element, h_i is the average vertical height of the ith element, and d_i is the horizontal width at h_i. A detailed description of the algorithm operations is given elsewhere.[5] The change in the bubble volume per unit time is considered to be the interstitial orifice gas flow rate. It is the true volumetric gas flow rate through the orifice during the bubbling stage. An average interstitial orifice flow rate is reported because the driving force for the flow fluctuates with time.[5,22]

Results and Discussion

Effect of Orifice Surface Roughness. Liquid weeping rate is defined as the volume of liquid weeping into the plenum per unit orifice area per unit time of operation. Hence, it can be considered as the average liquid velocity passing through the orifice into the plenum. The effect of orifice surface roughness on the liquid weeping rate at a superficial orifice gas velocity range of 147−703 cm/s are shown in Figure 5. The effect of superficial orifice gas velocity on the liquid weeping rate is consistent among all the orifice surface roughnesses. The liquid weeping rate increases initially and then decreases with an increase in the superficial orifice gas velocity. The effect of the orifice surface roughness on the liquid weeping rate, however, depends on the superficial orifice gas velocity. At low superficial orifice gas velocities, an increase in the orifice surface roughness decreases the liquid weeping rate. It can be seen from Figure 6a that the relationship between the liquid weeping rate and the orifice surface roughness at low superficial orifice gas velocities is approximately linear. On the contrary, an increase in the orifice surface roughness increases the liquid weeping rate at high superficial orifice gas velocities. The relationship between the liquid weeping rate and the orifice surface roughness still remains approximately linear at high superficial orifice gas velocities as shown in Figure 6b. In brief, a high orifice surface roughness suppresses liquid weeping at low superficial orifice gas velocities while a high orifice surface roughness promotes liquid weeping at high superficial orifice gas velocities.

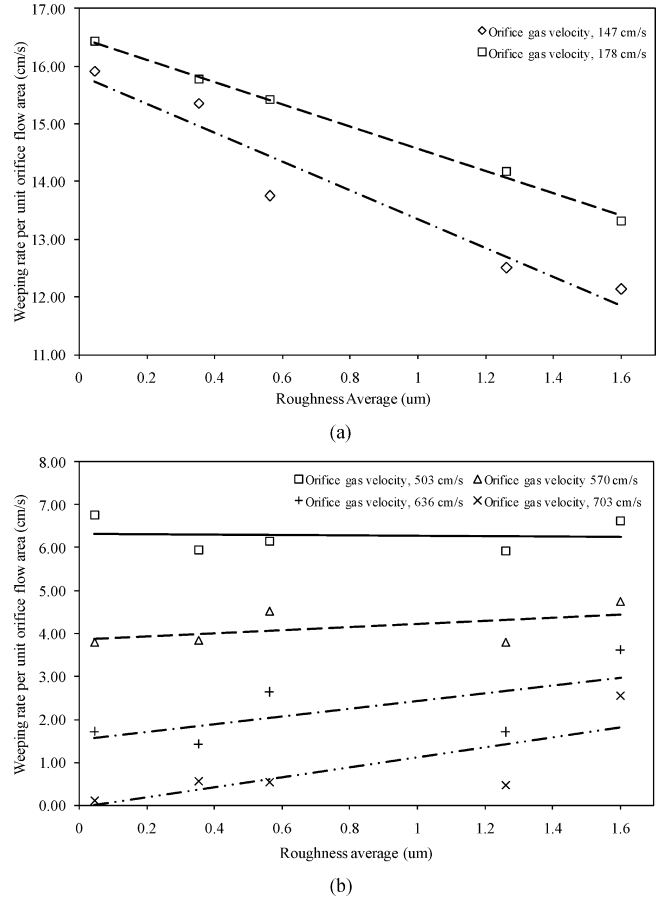

Figure 6. Relationship between liquid weeping rate and surface roughness (RA): (a) at low superficial orifice gas velocities; (b) at high superficial gas velocities.

In order to determine the underlying effect of the orifice surface roughness on the liquid weeping rate, additional analyses are performed by applying an image analysis algorithm on the high-speed image sequences of the bubbling and liquid weeping process. The time distribution of the various stages (bubbling stage, gas−liquid interface movement stage, weeping stage, and bridging stage) in a cycle and the detachment bubble volume are determined using the algorithm. The Reynolds number of the flow at the bubbling and the weeping stages and the plenum pressure fluctuation are also examined. The Reynolds number is defined as:

$$\mathrm{Re} = \frac{U_o \rho D_o}{\mu} \tag{2}$$

where ρ is the fluid density, μ is the fluid viscosity, D_o is the orifice diameter, and U_o is the interstitial velocity of the respective fluid. For Re during the bubbling stage, U_o is the average interstitial orifice gas velocity, calculated by dividing the average interstitial orifice gas flow rate during the bubbling stage with the orifice cross-sectional area. For Re during the weeping stage, U_o is the average interstitial orifice liquid velocity, calculated by dividing the weeping rate by the time fraction of the liquid weeping stage in the entire bubbling and liquid weeping cycle.

Effect of Orifice Surface Roughness on Liquid Weeping at Low Superficial Orifice Gas Velocities. The RAs of 1.601 and 0.046 are the extrema surface roughnesses considered in

Table 3. Comparison of the Reynolds Number of the Flow at the Bubbling and Weeping Stages, the Detachment Bubble Volume, and the Average Interstitial Orifice Gas Flow Rate at Orifice Surface Roughness of 1.601 and 0.046 at a Superficial Orifice Gas Velocity of 265 cm/s

orifice surface roughness (μm)	Reynolds number		detachment bubble volume (cm^3)	average interstitial orifice gas flow rate (cm^3/s)
	bubbling	weeping		
1.601	2386	1547	$9.90 \leq 11.01(avg) \leq 12.12$	140.56
0.046	2721	1522	$11.27 \leq 13.24(avg) \leq 15.78$	160.29

this study. A comparison of the bubbling and weeping phenomena at these two orifice surface roughnesses would be beneficial to the understanding of the observed difference in the liquid weeping rate. It can be seen from Figure 5 that within the low superficial orifice gas velocities range of 147−372 cm/s, the RA 0.046 orifice has a substantially higher liquid weeping rate than the RA 1.601 orifice. Therefore, a superficial orifice gas velocity of 265 cm/s is chosen for further in-depth analysis.

An immediate interpretation of the difference in the liquid weeping rate is expected to come from the higher friction loss in the liquid flow through the RA 1.601 orifice due to the higher surface roughness. However, the role of surface roughness in friction loss is only pronounced in the transition and turbulent flow regimes.[21] The Reynolds number for the liquid flow through the orifice during the weeping stage is tabulated in Table 3. A Reynolds number of 1500 for the liquid flow indicates that the liquid weeping is in the laminar flow regime. In the laminar flow regime, friction loss is independent of surface roughness.[21] Even though some studies found that surface roughness can have an effect on the friction loss under the laminar flow regime, it tends to be valid only under microchannel flow conditions.[23] Therefore, it is likely that the friction loss of the liquid flow through the orifice is not the governing mechanism of the change in liquid weeping with the orifice surface roughness.

The image sequence of a complete bubbling and weeping cycle at the RA 1.601 and the RA 0.046 orifices are illustrated in Figures 7 and 8, respectively. Four distinct stages,[5] namely (a) bubbling, (b) gas−liquid interface movement, (c) weeping, and (d) bridging can be observed in the bubbling and weeping cycle at both orifices. The bubbling, weeping, and bridging take place in a similar way for both orifices. However, a comparison between Figures 7b and 8b shows that the gas−liquid interface movement stages at these two orifices are different. Right after the bubble detachment at the RA 1.601 orifice, the gas−liquid interface continues to expand and forms a small secondary bubble. The gas−liquid interface only starts to move toward the plenum upon the detachment of the secondary bubble. On the other hand, no secondary bubble formation is observed at the RA 0.046 orifice. Table 4 gives a comparison of the time distribution of the various stages in a cycle between the two orifices. It indeed indicates that the gas−liquid interface movement time per cycle is higher in the RA 1.601 orifice than that in the RA 0.046 orifice. As the gas−liquid interface at the RA 1.601 orifice expands and form a secondary bubble, it extends the time of the gas−liquid interface movement stage. However, the difference in the gas−liquid interface movement time is small compared to the difference in the liquid weeping time between the two orifices. Therefore, it is anticipated that the orifice surface roughness affects the liquid weeping by involving other mechanisms.

The critical plenum pressure, $P_{c,critical}$, beyond which the liquid weeping ceases, may also affect the liquid weeping rate. The critical plenum pressure is a function of the hydrostatic presssure at the top of the orifice, the friction loss across the orifice, and the pressure generated by the liquid surface tension acting at the orifice during liquid weeping. The hydrostatic pressure depends on the liquid height in the column while the pressure generated by the liquid surface tension depends on the orifice diameter and the liquid surface tension.[9,22,24] As a fixed liquid height is maintained in the column and the orifice diameter, gas phase, and liquid phase

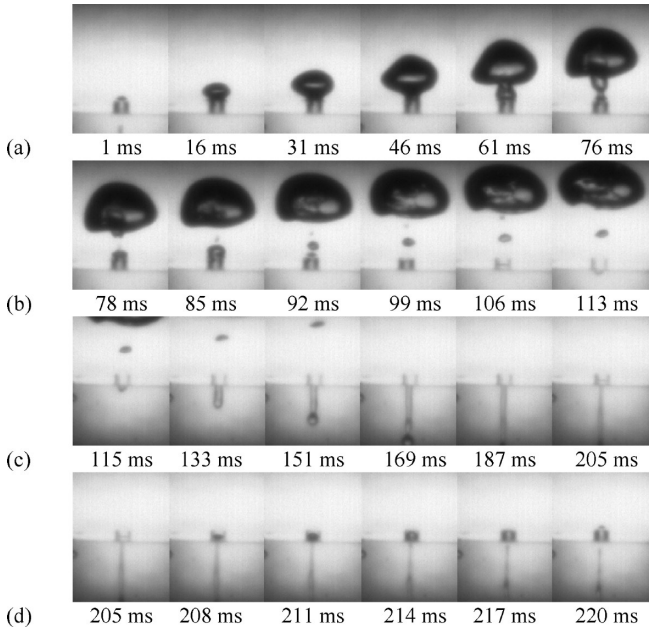

Figure 7. Illustration of bubbling and weeping cycle at the RA 1.601 orifice at a superficial orifice gas velocity of 265 cm/s: (a) bubbling stage, (b) gas−liquid Interface movement stage, (c) liquid weeping stage, and (d) bridging stage.

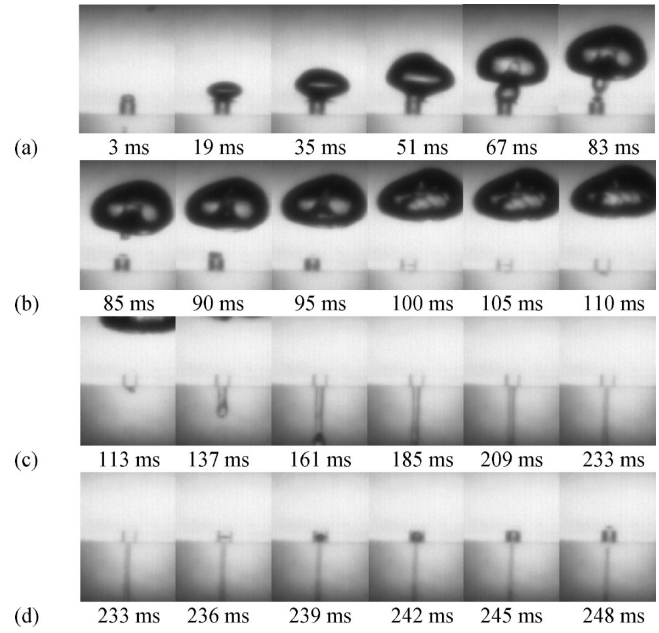

Figure 8. Illustration of bubbling and weeping cycle at the RA 0.046 orifice at a superficial orifice gas velocity of 265 cm/s: (a) bubbling stage, (b) gas−liquid Interface movement stage, (c) liquid weeping stage, and (d) bridging stage.

Table 4. Comparison of the Time Distribution of Various Stages in a Cycle between the Orifice Surface Roughness of 1.601 and 0.046 at a Superficial Orifice Gas Velocity of 265 cm/s

	time distribution of various stages in a cycle				
orifice surface roughness	cycle (ms)	bubbling (ms)	interface movement (ms)	weeping (ms)	bridging (ms)
1.601	224.55	78.33	36.78	93.11	16.33
0.046	250.40	82.60	28.80	122.50	16.50

are the same for all the experiments, the hydrostatic pressure and the pressure generated by the liquid surface tension can be considered to be the constant. As indicated in the earlier paragraph, the liquid flow conditions in the orifice are likely to be in the laminar flow regime, the friction loss would be independent of the surface roughness. Thus, the critical plenum pressure should be the same for both orifices.

The driving force for liquid weeping depends on the pressure difference between the top of the orifice and the plenum. While the pressure at the top of the orifice is essentially the hydrostatic pressure which depends on the liquid level in the column, it can be considered constant. On the other hand, the plenum pressure is associated with a number of factors. The previous studies describe the plenum pressure decreases during the bubbling stage.[1,5,22] The plenum pressure would reach a minimum at the moment of bubble detachment. This minimum plenum pressure should decrease with an increase in the detachment bubble volume. Table 3 shows that the detachment bubble volume at the RA 1.601 orifice is smaller than that at the RA 0.046 orifice. This result is indeed in agreement with the plenum pressure fluctuation measurement shown in Figure 9 that the RA 1.601 orifice has a higher minimum plenum pressure than the RA 0.046 orifice. For a constant pressure at the top of the orifice, a higher minimum plenum pressure at the bubble detachment would yield a lower driving force for liquid weeping. Therefore, the driving force for liquid weeping at the RA 1.601 orifice is lower than that at the RA 0.046 orifice. The difference in the detachment bubble volumes for both orifices is believed to be a consequence of the friction loss associated with the gas flow through the orifice during the bubbling stage. Table 3 shows that the Reynolds number for the gas flow through the orifice during the bubbling stage is over 2300. It is higher than the literature Reynolds number of 1760−2300 for the transition flow regime in pipe flow.[25,26] Friction loss is found to depend on both surface roughness and Reynolds number in the transition flow regime.[21] In addition,

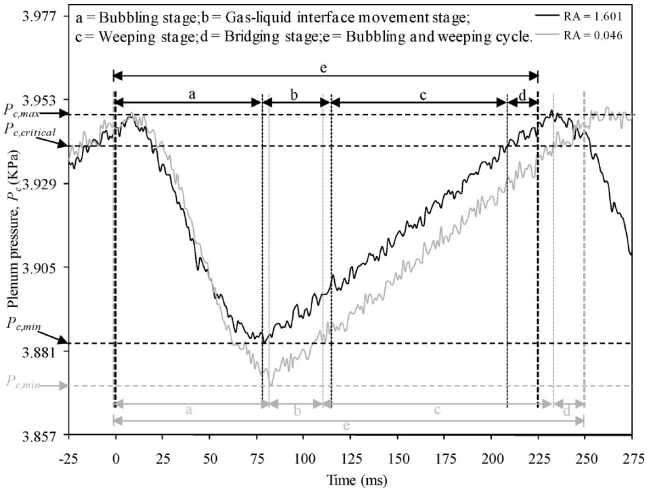

Figure 9. Comparison of plenum pressure fluctuation between the orifices with RAs of 1.601 and 0.046 at a superficial orifice gas velocity of 265 cm/s.

Table 5. Forces Acting on a Bubble from an Orifice at Bubble Detachment

forces (direction)	expression	effect on the detachment bubble volume with a reduction of Q_o
F_B(upward)	$v_b(\rho_l - \rho_g)g$	unchanged
F_M(upward)	$\rho_g \frac{Q_o^2}{A_o}$	increase
F_D(downward)	$3\mu_L \frac{Q_o}{d_b}$	decrease
F_o(downward)	$\pi D_o \sigma \cos\gamma$	unchanged
F_{Basset}(downward)	$3d_b^2\sqrt{\pi\rho_l\mu_l}\frac{du}{dt}$	decrease
$F_{I,g}$(downward)	$\frac{d}{dt}\left[\rho_g \frac{v_b}{A_b} Q_o\right]$	decrease
$F_{I,l}$(downward)	$\varsigma\frac{d}{dt}\left[\rho_l \frac{v_b}{A_b} Q_o\right]$	decrease

the low orifice thickness suggests that the entire flow inside the orifice would be in the entrance region. Studies have indicated that the friction loss at the entrance region is larger than the fully developed region in the laminar flow regime due to intense mixing and momentum transfer.[27−31] The low orifice thickness is believed to enhance the effect of surface roughness on the friction loss at the transition flow regime. The experimentally measured average interstitial orifice gas flow rate indeed indicates a lower gas flow at the RA 1.601 orifice than that at the RA 0.046 orifice, which is a result of the higher friction loss at the RA 1.601 orifice at the bubbling stage.

The effect of orifice surface roughness on the detachment bubble volume can also be obtained by a comparison of the forces acting on the bubble at the moment of bubble detachment. The expression for all the forces acting on the bubble are shown in Table 5.[22] The upward forces include the buoyancy force (F_B) and the gas momentum force (F_M). The downward forces include the surface tension force (F_σ), the liquid drag force (F_D), the Basset force (F_{Basset}), the gas inertial force ($F_{I,g}$), and the liquid inertial force ($F_{I,l}$). The sum of the upward forces just exceeds the sum of the downward forces at the moment of bubble detachment. Therefore, an analysis on the effect of orifice surface roughness on the upward and the downward forces can show the corresponding effect on the detachment bubble volume. In other words, a decrease in the upward forces would yield a larger detachment bubble volume, and a decrease in the downward forces would yield a smaller detachment bubble volume. The main effect of orifice surface roughness on the forces would be on the change in the interstitial orifice gas flow rate, Q_o due to friction loss. Since F_B is governed by the bubble

Table 6. Comparison of the Reynolds Number of the Flow at the Bubbling and Weeping Stages, the Detachment Bubble Volume, and the Average Interstitial Orifice Gas Flow Rate for Orifice Surface Roughness of 1.601 and 0.046 at a Superficial Gas Velocity of 636 cm/s

orifice surface roughness (μm)	Reynolds number		detachment bubble volume (cm^3)	average interstitial orifice gas flow rate (cm^3/s)
	bubbling	weeping		
1.601	3210	948	$10.85 \leq 15.07$ (avg) ≤ 18.94	189.10
0.046	3639	1102	$15.86 \leq 17.46$ (avg) ≤ 19.76	214.39

volume only, it is not directly affected by the orifice surface roughness. A reduction in Q_o will reduce F_M and yield a larger bubble volume. Among the downward forces, other than F_σ (which is independent of Q_o), F_D, $F_{I,g}$, and $F_{I,l}$ all decrease with a reduction in Q_o. F_{Basset} decreases with a reduction in Q_o but increases with bubbling growth time t when Q_o is reduced. Since F_{Basset} is proportional to $t^{0.5}$ and Q_o, the effect of Q_o should dominate. Thus, F_{Basset} also decreases with a reduction in Q_o. The analysis indicates that there is a counteracting effect between F_M and all the downward forces on the detachment bubble volume. An estimation of the relative magnitude of these forces would be necessary. On the basis of the experimental measurements, average Q_o is reduced from 160.29 to 140.56 cm^3/s when the orifice surface roughness is changed from 0.046 RA to 1.601 RA. The corresponding decrease in $F_{I,l}$ alone ($\sim 8.50 \times 10^{-4}$ N) is more than double the decrease in F_M ($\sim 3.64 \times 10^{-4}$ N). Thus, the change in the downward forces on the detachment bubble volume dominates that in the upward force, F_M. The result is in agreement with the literature finding that the influence of F_M on bubble formation is typically insignificant under low gas velocities or low gas density conditions.[22] As a result, an increase in orifice surface roughness for low superficial orifice gas velocities would reduce the detachment bubble volume. This reduction in detachment bubble volume then leads to a higher minimum plenum pressure and a lower driving force and eventually reduces the liquid weeping.

Effect of Orifice Surface Roughness on Liquid Weeping at High Superficial Orifice Gas Velocities. In contrast to the effect of orifice surface roughness on liquid weeping at low superficial orifice gas velocities, an increase in the orifice surface roughness increases the liquid weeping rate at high superifical orifice gas velocities. The effect of the orifice surface roughness on liquid weeping is reversed. As shown in Table 6, the Reynolds number of the liquid flow through orifice during liquid weeping is still under the laminar flow regime. The difference in the liquid weeping rate is again not governed by the friction loss during the liquid weeping stage.

Similarly, analysis is performed for the two extrema orifice surface roughnesses of RAs 1.601 and 0.046 at a superficial orifice gas velocity of 636 cm/s. Table 6 shows that the detachment bubble volume at both orifices fluctuates quite substantially at high superficial orifice gas velocities compared to that at low superifical orifice gas velocities. The detachment bubble volume at the RA 0.046 orifice is generally larger than that at the RA 1.601 orifice. It suggests that the RA 0.046 orifice should have a higher liquid weeping rate than that of the RA 1.601 orifice, which is contradictory to the liquid weeping rate observed.

An examination of the high-speed images in Figures 10 and 11 indicates that two distinct bubbling and liquid weeping processes can be observed at the RA 0.046 orifice at a fixed superficial orifice gas velocity of 636 cm/s. Figure 10 shows the presence of the four distinct stages in a bubbling and weeping cycle when bubbling occurs. However, Figure 11 shows that there are interactions among three consecutive smaller bubbles and the occurrence of multiple bubble coalescence at the same superficial orifice gas velocity. The formation of the stem coalescence phenomenon demarcates the transition from the bubbling regime to the jetting regime[32] and prevents the liquid weeping phenomenon. The presence of bubble−bubble interactions enhances the upward force acting on the growing bubble and significantly reduces the detachment bubble volume. The plenum pressure fluctuation at the formation of stem coalescences is anticipated to have smaller magnitude and be more erratic than that at the formation of individual bubbles. As a matter of fact, the two types of pressure fluctuation signals are present at both orifices as indicated in Figure 12. However, the presence of the stem colescence phenomenon is more frequent at the RA 0.046 orifice than at the RA 1.406 orifice.

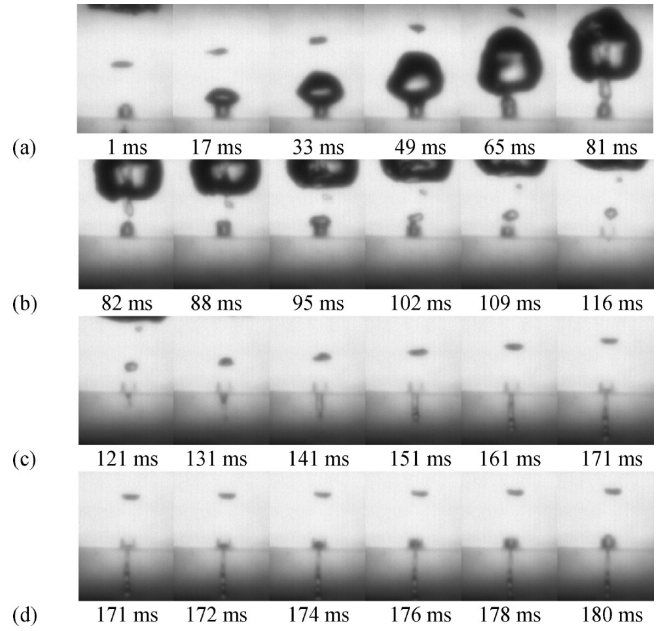

Figure 10. Illustration of individual bubble formation at the RA 0.046 orifice at a superficial orifice gas velocity of 636 cm/s: (a) bubbling stage, (b) gas−liquid interface movement stage, (c) liquid weeping stage, and (d) bridging stage.

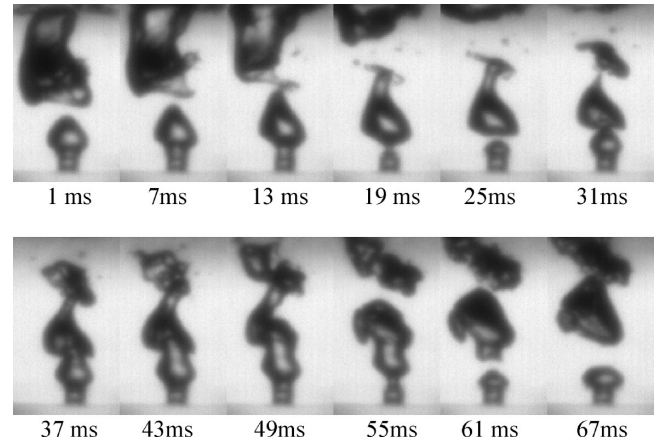

Figure 11. Illustration of the stem coalescence pheonomena at the RA 0.046 orifice at a superficial orifice gas velocity of 636 cm/s.

Table 7. Distribution of Individual Bubble Formation and Stem Coalescence Formation Based on the Analysis of the Plenum Pressure Fluctuation Signals for 30 s at the RA 1.601 and the RA 0.046 Orifices at a Superficial Orifice Gas Velocity of 636 cm/s

orifice surface roughness (μm)	individual bubble formation in 30 s		stem coalescence formation in 30 s	
	number of bubbles	duration (s)	number of bubbles	duration (s)
1.601	128	23.17	47	6.83
0.046	44	7.55	207	22.45

The plenum pressure fluctuations at various stages of bubbling/jetting transition were reported by Ruizuka et al.[33] At true bubbling regime where individual bubbles are formed, the pressure fluctuation is periodic. Upon an increase in the gas velocity approaching the bubbling/jetting transition, the plenum pressure fluctuation starts to exhibit unstable low amplitude bursts that can be identified as a continuous jet of gas (stem coalescence formation). As the gas velocity is further increased, the number of jetting bursts and their duration increases. Eventually the gas jet is stabilized and reaches the true jetting regime.[33] Therefore, the distribution of individual bubble formation and stem coalescence formation can give an indication of the relative nearness to the jetting regime. Table 7 shows the distribution (in terms of number of bubbles and duration) of individual bubble formation and stem coalescence formation based on the analysis of the plenum pressure fluctuation signals for 30 s. It indeed indicates that individual bubble formation is dominated at the RA 1.601 orifice while the stem coalescence formation is dominated at the RA 0.046 orifice. The literature reports a bubbling/jetting regime transition Reynolds number range of 3600−19 000 in an air−water system.[32−35] The Reynolds number of the bubbling stage listed in Table 6 indicates that the lower friction loss at the RA 0.046 orifice gives rise to a Reynolds number that falls within the range of the bubbling/jetting regime transition Reynolds number. Therefore, the effect of orifice surface roughness on liquid weeping at high superficial orifice velocities can be interpreted as follows: a reduction in the orifice surface roughness causes an increase in the instanteous orifice gas velocity so as to enable the transition to the jetting regime at a lower superficial gas velocity and reduce the liquid weeping rate.

Conclusion

The effect of orifice surface roughness on the liquid weeping phenomenon in a bubble column is studied over a wide range of superficial orifice gas velocities. It is found that the effect of orifice surface roughness on liquid weeping is governed by the bubbling behaviors at the orifice. At low superficial orifice gas velocities, an increase in orifice surface roughness reduces the interstitial orifice gas velocity and decreases the detachment bubble volume. As a result, the driving force for liquid weeping is reduced and liquid weeping is suppressed. When the orifice gas velocity is approaching the bubbling/jetting regime transition, an increase in orifice surface roughness causes a delay in the transition into the jetting regime and hence increases the liquid weeping. A modification of the orifice surface roughness is a possible solution to the reduction of liquid weeping. However, care should be taken when the operating gas velocity is close to the bubbling/jetting regime transition.

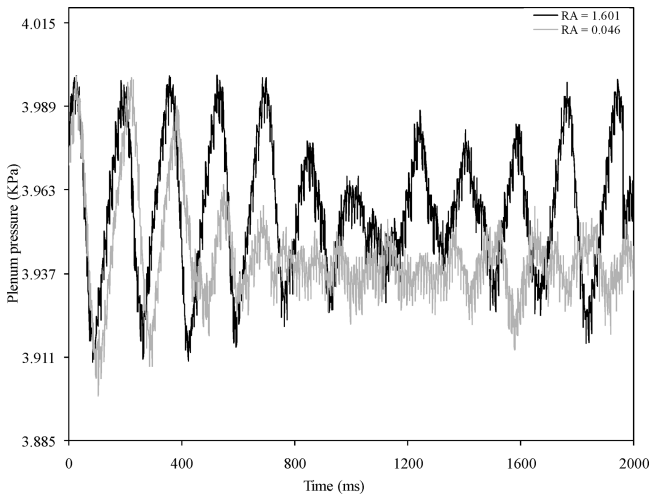

Figure 12. Comparison of plenum pressure fluctuation between RA 1.601 and RA 0.046 orifices at a superficial orifice gas velocity of 636 cm/s.

Acknowledgment

Support by AcRF Tier1 grant RG41/06 and A*STAR SERC grant 062 101 0035 is gratefully acknowledged.

Nomenclature

Notations

A_b = surface area of an emerging bubble
A_o = orifice flow area
d_b = overall bubble diameter
d_i = diameter of a disk formed by rotating horizontal element
D_o = orifice diameter
F_B = effective buoyancy force
F_{Basset} = basset force
F_D = liquid drag force
$F_{I,g}$ = gas inertial force
$F_{I,l}$ = liquid inertial force
F_M = gas momentum force
F_σ = surface tension force
g = gravitational constant
h = overall height
h_i = average vertical height of the ith differential element
Δh_i = vertical height of the ith element
N = number of horizontal differential elements
P_c = plenum pressure
$P_{c,critical}$ = critical plenum pressure
$P_{c,max}$ = maximum plenum pressure
$P_{c,min}$ = minimum plenum pressure
Q_o = interstitial orifice gas flow rate during the bubbling stage
t = time
u = rise velocity of emerging bubble
U_o = interstitial orifice velocity
v_b = volume of an emerging bubble

Greek Letters

μ_l = liquid viscosity
γ = contact angle between bubble surface and orifice
ρ_g = gas density
ρ_l = liquid density
σ = surface tension
ς = coefficient of liquid inertial force

Literature Cited

(1) Akagi, Y.; Okada, K.; Kosaka, K.; Takahashi, T. Liquid weeping accompanied by bubble formation at submerged orifices. *Ind. Eng. Chem. Res.* **1987**, *26*, 1546.

(2) McCann, D. J.; Prince, R. G. H. Bubble formation and weeping at a submerged orifice. *Chem. Eng. Sci.* **1969**, *24*, 801.

(3) Miyahara, T.; Iwata, M.; Takahashi, T. Bubble formation pattern with weeping at a submerged orifice. *J. Chem. Eng. Jpn.* **1984**, *17*, 592.

(4) Peng, W. L.; Yang, G.; Fan, L.-S. Experimental studies of liquid weeping and bubbling phenomena at submerged orifices. *Ind. Eng. Chem. Res.* **2002**, *41*, 1666.

(5) Hossain, M. I.; Pang, S. Q.; Pang, Q. X.; Yanhui, Y.; Lau, R. Study of liquid weeping at a tapered orifice in a bubble column reactor by computer aided image analysis algorithm. *Ind. Eng. Chem. Res.* **2010**, *49*, 3840.

(6) Klug, P.; Vogelpohl, A. Bubble formation with superimposed liquid motion at single-hole plates and sieve plates. *Ger. Chem. Eng.* **1983**, *6*, 311.

(7) Che, D. F.; Chen, J. J. J. Bubble formation and liquid weeping at an orifice submerged in a liquid. *Chem. Eng. Technol.* **1990**, *62*, 947.

(8) Lockett, M. J.; Banik, S. Weeping from sieve trays. *Ind. Eng. Chem. Process Des. Dev.* **1986**, *25*, 561.

(9) Zhang, W.; Tan, R. B. H. A model for bubble formation and weeping at a submerged orifice. *Chem. Eng. Sci.* **2000**, *55*, 6243.

(10) Zhang, W.; Tan, R. B. H. A model for bubble formation and weeping at a submerged orifice with liquid cross-flow. *Chem. Eng. Sci.* **2003**, *58*, 287.

(11) Gennes, P. G. D. Wetting: statics and dynamics. *Rev. Mod. Phys.* **1985**, *57*, 827.

(12) Marmur, A. Wetting on hydrophobic rough surfaces: to be heterogeneous or not to be. *Langmuir* **2003**, *19*, 8343.

(13) Bico, J.; Thiele, U.; Quere, D. Wetting of textured surfaces. *Colloids Surf., A* **2002**, *206*, 41.

(14) Visser, J. Van der Waals and other cohesive forces affecting powder fluidization. *Powder Technol.* **1989**, *58*, 1.

(15) Gotzinger, M.; Peukert, W. Particle adhesion force distributions on rough surfaces. *Langmuir* **2004**, *20*, 5298.

(16) Beach, E. R.; Tormoen, G. W.; Drelich, J.; Han, R. Pull-off force measurements between rough surfaces by atomic force microscopy. *J. Colloid Interface Sci.* **2002**, *247*, 84.

(17) Li, Q.; Rudolph, V.; Weigl, B.; Earl, A. Interparticle van der waals force in powder flowability and compactibility. *Int. J. Pharm.* **2004**, *280*, 77.

(18) Wassermann, P.; Kloker, M. Mechanisms and passive control of cross flow-vortex-induced transition in a three-dimensional boundary layer. *J. Fluid. Mech.* **2002**, *456*, 49.

(19) Katoh, K.; Choi, K.-S.; Azuma, T. Heat-transfer enhancement and pressure loss by surface roughness in turbulent channel flows. *Int. J. Heat Mass Transfer* **2000**, *43*, 4009.

(20) Picioreanu, C.; Van Loosdrecht, M. C. M.; Heijnen, J. J. A theoretical study on the effect of surface roughness on mass transport and transformation in biofilms. *Biotechnol. Bioeng.* **2000**, *68*, 355.

(21) Moody, L, F.; Princeton, N. J. Friction factors for pipe flow. *Trans. ASME* **1944**, 671.

(22) Yang, G. Q.; Luo, X.; Lau, R.; Fan, L.-S. Bubble formation in high-pressure liquid-solid suspensions with plenum pressure fluctuation. *AIChE J.* **2000**, *46*, 2162.

(23) Gloss, D.; Herwig, H. Wall roughness effects in laminar flows. *Exp. Fluids* **2010**, *49*, 461.

(24) Levich, V. G. *Physicochemical hydrodynamics*; Prentice Hall: Englewood Cliffs, NJ, 1962; p 378.

(25) Kerswell, R. R. Recent progress in understanding the transition to turbulence in a pipe. *Nonlinearity* **2005**, *18*, 17.

(26) Eckhardt, B.; Schneider, T. M.; Hof, B.; Westerweel, J. Turbulence transition in pipe flow. *Annu. Rev. Fluid Mech.* **2007**, *39*, 447.

(27) Astarita, G.; Greco, G. Excess pressure drop in laminar flow through sudden contraction. *Ind. Eng. Chem. Fund.* **1968**, *7*, 27.

(28) Schmidt, F. W.; Zeldin, B. Laminar Flows in Inlet Sections of Tubes and Ducts. *AIChE J.* **1969**, *15*, 612.

(29) Singh, M. P. Entry flow in a curved pipe. *J. Fluid Mech.* **1974**, *65*, 517.

(30) Chang, H. K.; Mortola, J. P. Fluid dynamic factors in tracheal pressure measurement. *J. Appl. Physiol.* **1981**, *51*, 218.

(31) Singh, R. P.; Nigam, K. K.; Mishra, P. Developing and fully developed turbulent flow through annuli. *J. Chem. Eng. Jpn.* **1980**, *13*, 349.

(32) Wraith, A. E.; Chalkley, M. E. Tuyere Injection for Metal Refining. In *Advances in Extractive Metallurgy*; Jones, M. J., Ed.; IMM: London, 1977; pp 27−33.

(33) Ruzicka, M. C.; Drahos, J.; Zahradnik, J.; Thomas, N. H. Intermittent transition from bubbling to jetting regime in gas-liquid two phase flows. *Int. J. Multiphase Flow.* **1997**, *23*, 671.

(34) Hoefele, E. O.; Brimacombe, J. K. Flow Regimes in Submerged Gas Injection. *Metall. Mater. Trans. B* **1979**, *10B*, 631.

(35) Liu, M. Y.; Hu, Z. D. Chaos Bubbling in Gas-liquid Two-Phase Bubble Column with a Single Orifice. *J. Chem. Ind. Eng. (China)* **2000**, *51*, 338.

Received for review May 29, 2010
Revised manuscript received November 2, 2010
Accepted November 12, 2010

IE101182X